Nanoscale

Cite this: *Nanoscale*, 2011, **3**, 1592

www.rsc.org/nanoscale

PAPER

Molecular level studies on binding modes of labeling molecules with polyalanine peptides†

Xiaobo Mao, Chenxuan Wang, Xiaojing Ma, Min Zhang, Lei Liu, Lan Zhang, Lin Niu, Qindao Zeng, Yanlian Yang* and Chen Wang*

Received 21st October 2010, Accepted 5th December 2010
DOI: 10.1039/c0nr00782j

In this work, the binding modes of typical labeling molecules (thioflavin T (ThT), Congo red (CR) and copper(II) phthalocyanine tetrasulfonic acid tetrasodium salt ($PcCu(SO_3Na)_4$)) on pentaalanine, which is a model peptide segment of amyloid peptides, have been resolved at the molecular level by using scanning tunneling microscopy (STM). In the STM images, ThT molecules are predominantly adsorbed parallel to the peptide strands and two binding modes could be identified. It was found that ThT molecules are preferentially binding on top of the peptide strand, and the mode of intercalated between neighboring peptides also exists. The parallel binding mode of CR molecules can be observed with pentaalanine peptides. Besides the binding modes of labeling molecules, the CR and $PcCu(SO_3Na)_4$ display different adsorption affinity with the pentaalanine peptides. The results could be beneficial for obtaining molecular level insight of the interactions between labeling molecules and peptides.

Introduction

The formation of β-sheet-rich amyloid has attracted extensive attention due to its association with a number of neurodegenerative processes.[1,2] The accumulation of intracellular amyloid-like aggregates by mutant proteins is the hallmark of two groups of codon reiteration disorders, for which there are currently few treatment options. An example is the Huntington's disease that is caused by polyglutamine repeats resulting from CAG trinucleotide repeat mutations. Another example could be found in the oculopharyngeal muscular dystrophy (OPMD).[3–5] OPMD is caused by the abnormal expansion of a $(GCG)_n$ repeat coding the polyalanine (polyA) peptide. Polyalanine stretches may cause cytotoxicity through mitochondrial dysfunction[4,6] and the exact mechanism responsible for its toxicity in OPMD is still unknown. By using X-ray diffraction (XRD) techniques, alanine-rich domains of prions are also reported to be the core domains of the amyloid formation due to the strong van der Waals interactions between polyalanines, such as SHa106-122 (KTNMKHMAGAAAAGAVV) and similar fragments.[7–11]

Investigations on amyloid fibrillation kinetics are crucial in understanding the fibril formation mechanisms and for examination of drugs to inhibit amyloid formation.[12] The molecular dynamics simulations (MD) on kinetics of fibril formation by polyalanine peptides suggested a conformational conversion process in which small amorphous aggregates → β-sheets → ordered nucleus → subsequent rapid growth of a small stable fibril or protofilament.[13–15]

The soluble model β-sheet complexes, polyalanine-based peptides, have also been designed for studying the β-sheet conformation in neurodegenerative disorders.[11,16] Among the most commonly used and convenient methods for the measurement of amyloid fibrillation formation and its kinetics are fluorescent and birefringent detections by using two kinds of representative dye molecules, thioflavin T (ThT) and Congo red (CR).[12,17–19] Many efforts have been made for studying the interactions between dye molecules and amyloid peptides, the underlying specific binding modes and fluorescence enhancement mechanisms.[20,21] A length-dependent effect has been reported for analyzing β-sheet formed by polyalanines with fluorescent method by using ThT assay.[22] The binding affinities of CR for amyloid-β and amylin fibrils vary considerably, and certain metal ions (Cu^{2+}, Ni^{2+}, Cd^{2+}) could change the affinity significantly.[23] The affinity of ThT to common β-sheet structures also gives rise to the interest for developing inhibiting species for treating amyloid diseases.[24,25] As another widely used labeling agent, CR has also been proved to reduce amyloid aggregation and cell death in cell models of OPMD and amyloid diseases.[24,26] Another kind of labeling molecules, phthalocyanine (Pc) and its derivatives, have also been suggested to bind to amyloid peptide, which could affect the amyloid formation and the related cytotoxicity.[27,28] To unveil the interactions between dye molecules and amyloid peptides at the molecular level, it is essential to develop the detection methods for studying the structural characteristics of amyloids under various conditions.

National Center for Nanoscience and Technology, Beijing, 100190, China. E-mail: yangyl@nanoctr.cn; wangch@nanoctr.cn; Fax: +86-10-62656765; Tel: +86-10-82545559 (Yang YL); +86-10-82545561 (Wang C)

† Electronic supplementary information (ESI) available. See DOI: 10.1039/c0nr00782j

A number of techniques have been applied to gain insights of the specificity of the interactions between dye molecules and amyloid peptides, such as XRD,[12,29,30] fluorescence,[31] circular dichroism,[20] isothermal titration calorimetry,[12,20,32] confocal microscopy,[21] molecular dynamics simulations,[33,34] computational modeling based on the crystal results.[31,35] One of the proposed binding sites is in the central pore region of amyloid fibrils determined by small angle X-ray scattering and XRD.[12,29] Several reports have suggested that the possible binding site for dye molecules is in the "channels" formed by side chains of residues along the long fibril axis.[20,21,31,33,34] The binding sites in parallel configuration have also been proposed experimentally and theoretically.[30,33–35] It should be noted that considerable challenges for the proposed binding modes still remain because of the lacking of direct evidence from structural analysis in both crystallization and assembly states.

In recent studies on molecular adsorption and assembling processes, scanning tunneling microscopy (STM) has provided a helpful venue for studying biological molecules due to its high structural resolution and adaptability to various environments, including liquid-solid interfaces[36,37] and ultra-high vacuum conditions.[38,39] Recently STM has been applied to study the core regions of amyloid assemblies with molecular level resolutions.[40,41]

In this work, using the organic-peptide co-assembly of pentaalanine (H_2N-Ala-Ala-Ala-Ala-Ala-COOH) with a chaperon-like molecules, 4,4′-bipyridyl (4Bpy), we have studied the binding modes of labeling molecules, ThT, CR and phthalocyanine tetrasulfonates $PcCu(SO_3Na)_4$, by using STM. The labeling molecule ThT for amyloid stain are found to bind with pentaalanine peptide strands in parallel and two kinds of detailed binding modes for ThT could be identified. The parallel binding mode of CR molecules could also be identified by STM. Furthermore, the different adsorption affinity of CR and the Pc derivatives to the co-assembly of pentaalanine peptides and 4Bpy molecules could also be deduced.

Materials and methods

Synthetic peptides and labeling molecules

Pentaalanine, 4,4′-bipyridyl, Congo red, thioflavin T and copper(II) phthalocyanine tetrasulfonic acid tetrasodium salt (Scheme 1) were obtained from Sigma-Aldrich Co. Ltd and used without further purification. The physical sizes of the molecules are provided correspondingly.

Sample preparation for STM studies

The lyophilized powder of pentaalanine (1 mg) and the solid powder of 4Bpy (1 mg) were dissolved in chromatographic grade acetonitrile (ACN) (1 mL) (ESI†). 1 μL solution of the mixture with pentaalanine and 4Bpy were deposited on highly oriented pyrolytic graphite (HOPG) immediately after mixing. STM experiments were performed after 1 h the solvent ACN was completely evaporated from the HOPG surface. The labeling molecules were firstly mixed with the solutions of pentaalanine and 4Bpy. In the experiments, two concentrations (0.1 mg mL^{-1}, 1 mg mL^{-1}) of the ThT molecules have been used. The concentration of CR is 0.1 mg mL^{-1}, and the concentration of $PcCu(SO_3Na)_4$ is 0.1 mg mL^{-1}. 1 μL of mixed solution were deposited on HOPG surface, and followed by the similar procedure for the mixture of pentaalanine and 4Bpy.

STM measurements

STM experiments were performed in constant-current mode under ambient conditions (Nanoscope IIIA scanning probe microscope (SPM) system, Veeco, USA). The tips were mechanically formed Pt/Ir wire (80/20). The STM tunneling conditions are described in the corresponding figure captions. The experiments were repeated more than 5 times independently using different tips for reproducibility for different labeling molecules.

Statistical methods

The lengths of the peptide strands in STM images are measured by using the Nanoscope software. A step size of 0.325 nm for every residue are assumed in the statistical histogram of the length distribution of the peptide assemblies, which is fitted by Gaussian distribution. The measured lengths in the histograms represent the average value of the independent experiments. The number frequencies in the statistical results are all based on number of events.

Results and discussion

Scheme 1 presents the schematic structures of pentaalanine and 4Bpy for the peptide assemblies, ThT and CR for amyloid stains, and Pc tetrasulfonates $PcCu(SO_3Na)_4$ as amyloid formation modulator. Pentaalanine is a peptide with methyl side groups only. ThT molecule consists of a pair of benzothiazole and benzaminic rings freely rotating around the inter-ring C–C bond. ThT shows enhanced fluorescence at 482 nm when bound to amyloid fibrils, which can be used as a sensitive diagnosis tool for amyloidosis. CR is a secondary diazo dye, which is water soluble, yielding a red colloidal solution. Apple-green birefringence of CR under polarized light is indicative for the presence of amyloid fibrils. $PcCu(SO_3Na)_4$ is a multifunctional molecule, which can be excited by visible or near-infrared light in photodynamic therapy (PDT).[42]

Pentaalanine is a model peptide for amyloid studies due to its repeated sequential structure with only hydrophobic side groups and the high occurrence of alanine residues in the abnormal protein sequences.[3,7–9] The assembly of pentaalanine contains nearly continuous lamellae structures in STM images (Fig. S1 in the ESI†). It has been reported that one of the characteristic features is 0.47 nm for the distance of two neighboring strands in the cross-β-sheet structure.[52] In Fig. S1A, the marked distance covering 10 molecules is measured to be 4.7 ± 0.2 nm which is consistent with the previous results. Since high-resolution STM images could only be achieved for molecular species that are adsorbed stably under ambient conditions. The side groups of pentaalanine molecules can not be identified in our STM images due to its structural fluctuations.

In order to identify the terminal positions of the pentaalanine molecules in the assembly, directional noncovalent interactions derived from co-adsorbed chaperon-like molecules are introduced.[28,43,44] In the current study 4Bpy is introduced as

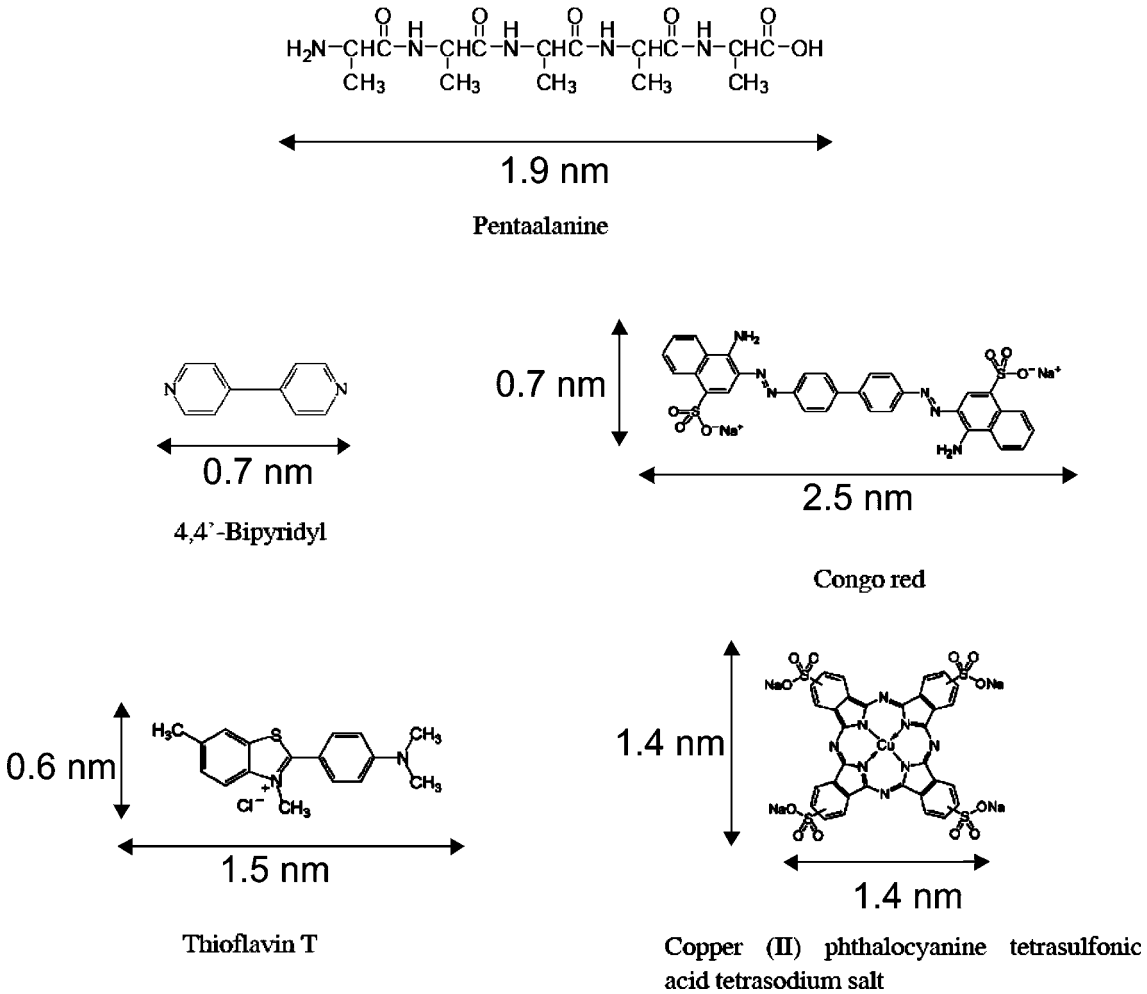

Scheme 1 Molecular structures of pentaalanine, 4,4′-bipyridyl (4Bpy), Congo Red (CR), thioflavin T (ThT), and copper(II) phthalocyanine tetrasulfonic acid tetrasodium salt ($PcCu(SO_3Na)_4$). The dimensions of the molecules are provided correspondingly.

a chaperon-like molecule to modulate the pentaalanine assembly. The STM image of the 4Bpy assembly (Fig. S2 in the ESI†) shows the characteristic close-packing assembly structures. Fig. 1A is a typical large-scale STM image of pentaalanine/4Bpy co-assembly on HOPG surface. 4Bpy with the conjugated π-electron structure can be associated with the bright features in linear array arrangement due to the higher electron density of states. The lamella bands with reduced contrast could be attributed to the pentaalanine. In the high-resolution STM image (Fig. 1B), the molecular dimensions of 4Bpy and pentaalanine could be determined quantitatively. It could be proposed that the formation of the heterogeneous peptide-organic assembly structure is facilitated by strong N···H–O hydrogen bond between N atom of 4Bpy and the carboxyl group of pentaalanine C-terminus, in which two pentaalanine stripes between the neighboring 4Bpy arrays are connected with a head-to-head configuration with N-terminus in the middle.[28,45] The stability of the hydrogen bond between 4Bpy and carboxyl group has been characterized by variable-temperature Fourier transform infrared spectroscopy (FTIR).[46] Molecular packing arrangements with different angles between molecular axis and lamellae direction are influenced by the competitive and collaborative interactions between different functional groups, which have been studied extensively.[47–49] The angle α between pentaalanine molecular axes and the stripe orientation is measured to be $32 \pm 2°$, which is associated with the hydrogen bond interaction between terminal functional groups.[45]

The distance between the neighboring pentaalanine molecules within one stripe is measured to be 4.7 ± 0.2 angstrom (Fig. S1, ESI†), indicative of a β-sheet-like structure of the pentaalanine assembly which has been suggested in the previous studies.[13–15] The *de novo* designed polyalanine-based peptides may undergo conformational changes from random coil conformations into soluble β-pleated-sheet motifs driven by hydrophobic interactions between the methyl groups of the alanine side chains.[16] In addition, fluorescence enhancement in ThT assay for the polyalanines also indicates the formation of β-sheet structures.[22] In this work, the lengths of the pentaalanine peptides are measured to be about 1.9 nm, as shown in Fig. 1C, which is in agreement with the expected length of the extended pentaalanine peptides.[40]

It has been suggested that amyloid aggregation is caused by backbone hydrogen bonds,[50] by maximizing the van der Waals interactions between side-chains,[51] and possible shape complementarities between neighboring molecules.[52,53] Then the introduction of 4Bpy molecules interacting with the C-terminus of pentaalanine molecules is unlikely to interfere with the related

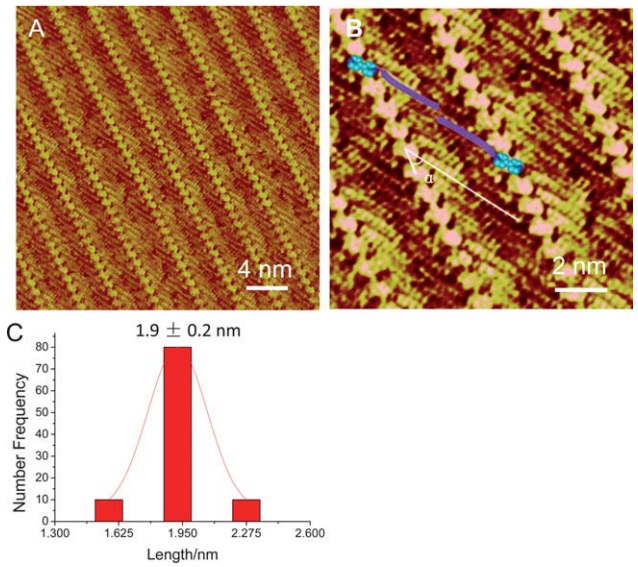

Fig. 1 (A, B) STM images of co-assembly of pentaalanine and 4Bpy. Tunneling conditions: $I = 323.5$ pA, $V = -846.6$ mV. (B) The angle α is referred to the angle between the peptide stripes and the peptide backbones, and the schematic illustration of the pentaalanine/4Bpy co-assembly is superimposed on the image. (C) The statistical histogram of the length of pentaalanine molecules. The average length is measured to be 1.9 ± 0.2 nm.

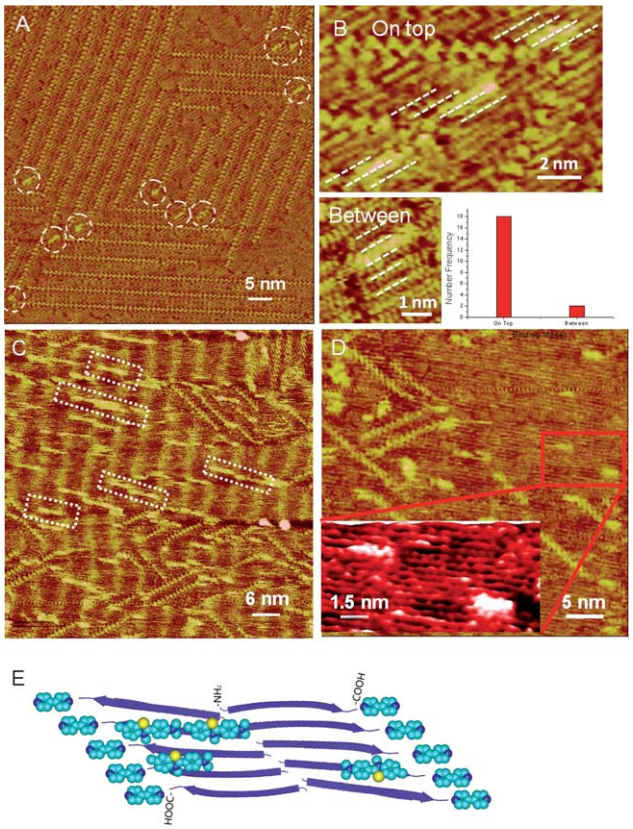

Fig. 2 (A) Large-scale STM image of ThT-atop-pentaalanine/4Bpy with lower ThT/peptide ratio. Tunneling conditions: $I = 402.8$ pA, $V = 422.1$ mV. White dashed circles highlight the adsorbed ThT molecules. (B) High-resolution STM images of the two binding modes of ThT molecules marked by white dotted lines and the histogram of statistical distribution of two binding modes. Tunneling conditions: $I = 402.8$ pA, $V = 422.1$ mV. (C) Large-scale STM image of ThT-atop-pentaalanine/4Bpy with higher ThT/peptide ratio. The white dashed rectangles represent the self-assembly of ThT molecules on pentaalanine assembly. The molecular long axes of ThT molecules are parallel to the pentaalanine strands. Tunneling conditions: $I = 314.3$ pA, $V = 821.8$ mV. (D) High-resolution STM images of ThT-atop-pentaalanine self-assembly. (E) The schematic illustration of the adsorption mode of ThT with pentaalanine/4Bpy co-assembly. The backbones of the peptide strands are represented in blue arrows. The atoms of ThT and 4Bpy in the illustration are colored by element type, cyan, blue and yellow colors for C, N and S atoms respectively.

binding modes of labeling molecules. The presence of the 4Bpy arrays with higher contrast further provides an indicator for identifying the binding modes of the labeling molecules on the peptide stripes (Fig. 1B).

Upon the introduction of ThT into the pentaalanine/4Bpy co-assembly, Fig. 2A reveals the randomly distributed bright features, which can be as attributed to the individual ThT molecules marked by white circles. In the large-scale STM image, the directions of the long axes of ThT molecules are predominantly adsorbed parallel to the orientations of the pentaalanine strands. In the high-resolution STM image (Fig. 2B), the ThT molecule is revealed as a hedge-shaped rod with bright contrast (~1.5 nm in length) with two parallel binding modes to the pentaalanine strands.[33,35] In the preferential binding mode, ThT molecules tend to bind on top of the pentaalanine peptide strands rather than intercalated between two neighboring peptide strands, as shown in the histogram of the statistical distribution of Fig. 2B. The observations of the two parallel binding modes are in accordance with the previously reported experimental and theoretical results.[30,33–35]

At higher ThT concentration, the adsorption of ThT oligomers with parallel orientation to the peptide strands could also be observed, as shown in white dashed rectangles in Fig. 2C. ThT assemblies on the pentaalanine peptides could be stably observed during STM experiments, suggesting the strong affinity of ThT to pentaalanine peptides.

Based on the measured length of ThT monomer (~1.5 nm) and the hedge-like features, the number of ThT molecules in the observed oligomers on pentaalanine assembly could be estimated as between 2 to 12, and the most probable value is 5 (Fig. S3 in the ESI†). Few ThT molecules could be observed binding on the 4Bpy site at the high concentration of ThT, which is also supportive to the consideration of high affinity of ThT molecules to pentaalanine strands. In addition, in the high-resolution STM images, as shown in Fig. 2D and the inset, the binding modes of ThT molecules to pentaalanine strands, can be clearly identified without 4Bpy molecules showing the predominant parallel orientations of ThT molecules to the pentaalanine strands. The binding modes of ThT molecules to pentaalanine/4Bpy co-assembly are schematically illustrated in Fig. 2E showing the preferential adsorption of ThT on peptide strands with parallel molecular orientations. The binding of ThT monomers and oligomers to pentaalanine assemblies could be ascribed to the nonspecific van der Waals interactions between the aromatic rings of ThT molecules and the hydrophobic peptide surface associated with the methyl side groups.

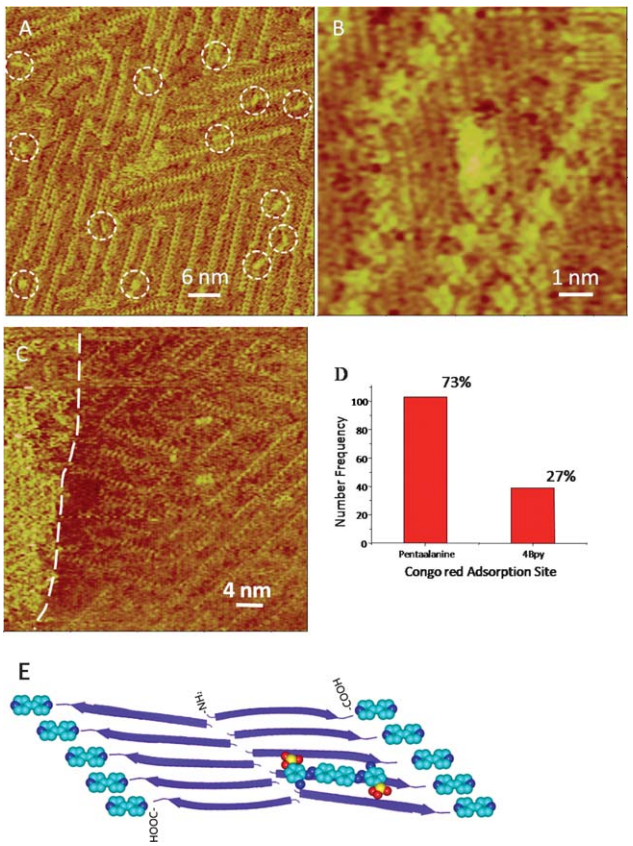

Fig. 3 (A) STM image of CR-atop-pentaalanine/4Bpy. Tunneling conditions: $I = 338.7$ pA, $V = 842.0$ mV. White dashed circles highlight the adsorbed CR molecules. (B) High-resolution STM images of CR-atop-pentaalanine/4Bpy. Tunneling conditions: $I = 338.7$ pA, $V = 842.0$ mV. (C) Self-assembled CR molecules on the pentaalanine/4Bpy co-assembly can be observed on the left side of the image indicated by the white dashed line. Tunneling conditions: $I = 305.2$ pA, $V = 609.1$ mV. (D) The histogram of the statistical distribution for CR molecules on two adsorption sites: pentaalanine and 4Bpy. (E) The schematic illustration of the adsorption mode of CR with pentaalanine/4Bpy co-assembly. All the legends and the colors are same to those in Fig. 2E, and the atoms in red is O.

In a parallel study with the CR as the labeling agent, similar features could be observed in the STM images. In Fig. 3A, CR molecules marked by white circles can be clearly recognized as rod-like features with higher contrast and random distribution on the co-assembly of pentaalanine/4Bpy. The molecular long axes of CR molecules are predominantly aligned with the axes of pentaalanine peptides as revealed by the high-resolution STM image (Fig. 3B), in agreement with the previously proposed parallel binding mode.[30,33–35] The location of CR molecules could be observed on top of the pentaalanine strands. In addition to the CR molecules bound to the peptide stripes, the CR molecules are also observed to self-assemble with distinctively different assembling characteristics, which are marked by the white dashed line in Fig. 3C. The affinity of CR to the pentaalanine surface could be related to the hydrophobic domain of amyloid peptides.[54–57] It was suggested that such interaction could affect the amyloid aggregation relating to amyloid toxicity.[24,26,58,59]

It should be noted that in these STM images of the organic-peptide co-assemblies, both pentaalanine peptides and 4Bpy are candidate binding sites for CR. From the histogram distribution of the statistical results for CR molecules on two adsorption sites, as shown in Fig. 3D, the adsorption site atop pentaalanine peptides is the preferential one according to the ratio of the adsorbates on two adsorption sites (pentaalanine *versus* 4Bpy) (103/39 or 73%: 27%). The preferential binding mode of CR atop pentaalanine peptide strands is schematically illustrated in Fig. 3E. In addition, a small portion of CR molecules could be immobilized in the trench regions between two stripes of pentaalanine peptides, and in the defects of the neighboring domains. The appearance of CR molecules seems to be discernible fluctuation both in shape and size, which could be a reflection of the difference in binding environment for the CR molecules.

Phthalocyanine (Pc) molecules have been used in PDT[60–63] experiments due to its opto-electrical properties,[64–66] and it has been suggested that Pc tetrasulfonates could suppress the amyloid formation and cytotoxicity. With the molecularly resolved assembled structure of pentaalanine peptide by using STM, it is possible to study the interaction between the peptides and Pcs. In the STM image (Fig. 4A), the Pc derivative, PcCu-$(SO_3Na)_4$ molecules, represented as bright square-like features, are distributed randomly in the co-assembly of pentaalanine/4Bpy. Two adsorption sites could also be observed, namely atop pentaalanine peptides and atop 4Bpy molecules. In the labeled white rectangle of Fig. 4A, one molecular chain formed by five $PcCu(SO_3Na)_4$ molecules can be clearly observed to adsorb at the domain boundary of pentaalanine assemblies. In the high-resolution STM image (Fig. 4B), it can be clearly identified that the $PcCu(SO_3Na)_4$ is adsorbed preferentially atop pentaalanine peptides. The preferential binding of $PcCu(SO_3Na)_4$ on peptide strands are illustrated in the histogram distribution (Fig. 4C) showing higher ratio of the adsorbate populations on two adsorption sites (pentaalanine *versus* 4Bpy) (77/7 or 92%: 8%). $PcCu(SO_3Na)_4$ can be considered as an aromatic moiety with planar structure and could interact with the pentaalanine assembly through van der Waals interactions. In addition, the introduction of the sulfonate groups to the Pc moiety is also critical for the interaction between the amyloid protein and Pc tetrasulfonates.[27] The electrostatic interaction between $-SO_3^-$ of $PcCu(SO_3Na)_4$ and $-NH_2$ of pentaalanine should also be taken into account in the interactions between $PcCu(SO_3Na)_4$ and pentaalanine, which gives rise to the more preferential site on pentaalanine surfaces (Fig. 4D). As to the 4Bpy molecules, it can be suggested that $PcCu(SO_3Na)_4$ and 4Bpy interact mainly *via* π–π interaction.

Due to the insolubility and non-crystalline nature of amyloid peptides, it is still a challenging task to determine the molecular-level structures of the binding configurations of labeling molecules. The study on the binding sites of labeling molecules by using STM is still at the preliminary stage. The current STM experiments are performed at liquid/solid interfaces, therefore, could be relevant to biological conditions of interests. The differences between the aggregation behavior of surface-bound peptides and that in solutions should also be explored.[67] It was suggested that dynamic exchanges of the adsorbed peptides with those in solutions could enable reversible conformational changes of the peptides.[68] Common to the peptide assemblies in solution and at various interfaces is that the molecule-molecule interactions are central to the assembling characteristics, which could cause amyloidal diseases.

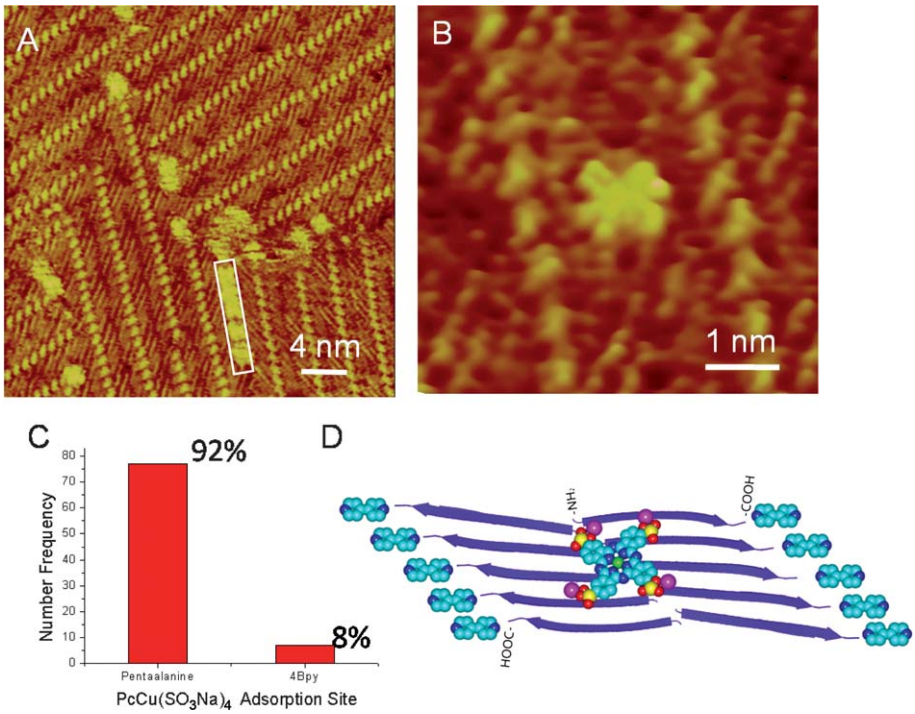

Fig. 4 (A and B) STM images of $PcCu(SO_3Na)_4$-atop-pentaalanine/4Bpy co-assembly. Tunneling conditions: $I = 363.2$ pA, $V = 660.1$ mV. The molecular chain of $PcCu(SO_3Na)_4$ at the domain boundary is highlighted with a white rectangle. (C) The histogram of the statistical distribution of $PcCu(SO_3Na)_4$ molecules on two adsorption sites, pentaalanine and 4Bpy. (D) The schematic illustration of the adsorption model of $PcCu(SO_3Na)_4$ with pentaalanine/4Bpy co-assembly. All the legends and colors are same to those in Fig. 2E, and the atoms in magenta and green are Na and Cu elements of $PcCu(SO_3Na)_4$.

The relevance between STM techniques and other important spectroscopic and microscopic methods on the binding behaviors of labeling molecules to various amyloid peptides is an interesting topic to pursue. It has been reported that the fluorescence efficiency are strongly dependent on the conformation of ThT and the deviation from planar conformation may lead to dramatic reduction of the fluorescence of ThT molecules.[69] Rigorous experimental and theoretical studies on the connection between the binding modes and enhanced fluorescence mechanism are keenly needed in the future efforts.

Conclusion

In summary, the binding modes of the labeling molecules to amyloid peptide model, pentaalanine, have been observed at the molecular level by using STM. In the co-assembly with the chaperon-like molecules, the C-termini of the pentaalanine peptides are recognized, providing a direct venue to identify various binding modes of labeling molecules. It has been identified that thioflavin T and Congo red could be bound parallel to the pentaalanine strands, and the CR and $PcCu(SO_3Na)_4$ molecules also tend to stay on pentaalanine peptide comparing to the lower affinity to 4Bpy binding sites. The identification of the binding behaviors could benefit the studies on the interactions between amyloid peptides and labeling molecular species.

Acknowledgements

This work was supported by the National Basic Research Program of China (2009CB930100, 2011CB932800) and Chinese Academy of Sciences (KJCX2-YW-M15). Financial support from National Natural Science Foundation of China (20911130229) and CAS Key Laboratory for Biological Effects of Nanomaterials & Nanosafety are also gratefully acknowledged. The authors would like to thank for the supplier of the programs, PyMOL[70] and NanoEngineer-1[71] for generation of the molecular models in Figures 2E, 3E and 3D.

References

1 D. J. Selkoe, Alzheimer's disease: Genes, proteins, and therapy, *Physiol. Rev.*, 2001, **81**, 741–766.
2 S. B. Prusiner, Prions, *Proc. Natl. Acad. Sci. U. S. A.*, 1998, **95**, 13363–13383.
3 U. Kuhn and E. Wahle, Structure and function of poly(A) binding proteins, *Biochim. Biophys. Acta, Gene Struct. Expr.*, 2004, **1678**, 67–84.
4 K. Toriumi, Y. Oma, Y. Kino, E. Futai, N. Sasagawa and S. J. Ishiura, Expression of polyalanine stretches induces mitochondrial dysfunction, *J. Neurosci. Res.*, 2008, **86**, 1529–1537.
5 B. Brais, Oculopharyngeal muscular dystrophy: A polyalanine myopathy, *Curr. Neurol. Neurosci. Rep.*, 2008, **9**, 76–82.
6 I. M. Nasrallah, J. C. Minarcik and J. A. Golden, A polyalanine tract expansion in Arx forms intranuclear inclusions and results in increased cell death, *J. Cell Biol.*, 2004, **167**, 411–416.
7 H. Inouye and D. A. Kirschner, X-ray diffraction analysis of scrapie prion: Intermediate and folded structures in a peptide containing two putative alpha-helices, *J. Mol. Biol.*, 1997, **268**, 375–389.
8 H. Inouye and D. A. Kirschner, Polypeptide chain folding in the hydrophobic core of hamster scrapie prion: Analysis by X-ray diffraction, *J. Neurochem.*, 1998, **70**, S7.
9 H. Inouye, J. Bond, M. A. Baldwin, H. L. Ball, S. B. Prusiner and D. A. Kirschner, Structural changes in a hydrophobic domain of

the prion protein induced by hydration and by Ala->Val and Pro->Leu substitutions, *J. Mol. Biol.*, 2000, **300**, 1283–1296.
10 J. T. Nguyen, H. Inouye, M. A. Baldwin, R. J. Fletterick, F. E. Cohen, S. B. Prusiner and D. A. Kirschner, X-Ray-Diffraction of scrapie prion rods and Prp peptides, *J. Mol. Biol.*, 1995, **252**, 412–422.
11 L. M. Shinchuk, D. Sharma, S. E. Blondelle, N. Reixach, H. Inouye and D. A. Kirschner, Poly-(L-alanine) expansions form core beta-sheets that nucleate amyloid assembly, *Proteins: Struct., Funct., Bioinf.*, 2005, **61**, 579–589.
12 M. Groenning, M. Norrman, J. M. Flink, M. van de Weert, J. T. Bukrinsky, G. Schluckebier and S. Frokjaer, Binding mode of Thioflavin T in insulin amyloid fibrils, *J. Struct. Biol.*, 2007, **159**, 483–497.
13 H. D. Nguyen and C. K. Hall, Kinetics of fibril formation by polyalanine peptides, *J. Biol. Chem.*, 2004, **280**, 9074–9082.
14 H. D. Nguyen, A. J. Marchut and C. K. Hall, Solvent effects on the conformational transition of a model polyalanine peptide, *Protein Sci.*, 2008, **13**, 2909–2924.
15 Y. Levy, J. Jortner and O. M. Becker, Solvent effects on the energy landscapes and folding kinetics of polyalanine, *Proc. Natl. Acad. Sci. U. S. A.*, 2001, **98**, 2188–2193.
16 S. E. Blondelle, B. Forood, R. A. Houghten and E. PerezPaya, Polyalanine-based peptides as models for self-associated beta-pleated-sheet complexes, *Biochemistry*, 1997, **36**, 8393–8400.
17 G. Kelenyi, Thioflavin S fluorescent and Congo Red anisotropic stainings in histologic demonstration of amyloid, *Acta Neuropathol.*, 1967, **7**, 336–348.
18 E. Gurr, 1965, Congo Red, in *Encyclopedia of Microscopic Stains*, pp. 140–141, Leonard Hill, London.
19 H. I. LeVine, Thioflavine T interaction with synthetic Alzheimer's disease beta-amyloid peptides: Detection of amyloid aggregation in solution, *Protein Sci.*, 2008, **2**, 404–410.
20 R. Sabate, I. Lascu and S. J. Saupe, On the binding of Thioflavin-T to HET-s amyloid fibrils assembled at pH 2, *J. Struct. Biol.*, 2008, **162**, 387–396.
21 M. R. H. Krebs, E. H. C. Bromley and A. M. Donald, The binding of thioflavin-T to amyloid fibrils: localisation and implications, *J. Struct. Biol.*, 2005, **149**, 30–37.
22 K. Giri, N. P. Bhattacharyya and S. Basak, pH-dependent self-assembly of polyalanine peptides, *Biophys. J.*, 2007, **92**, 293–302.
23 T. T. Ashburn, H. Han, B. F. Mc Guinness and P. T. Lansbury, Amyloid probes based on Congo Red distinguish between fibrils comprising different peptides, *Chem. Biol.*, 1996, **3**, 351–358.
24 V. Heiser, E. Scherzinger, A. Boeddrich, E. Nordhoff, R. Lurz, N. Schugardt, H. Lehrach and E. E. Wanker, Inhibition of huntingtin fibrillogenesis by specific antibodies and small molecules: Implications for Huntington's disease therapy, *Proc. Natl. Acad. Sci. U. S. A.*, 2000, **97**, 6739–6744.
25 C. I. Stains, K. Mondal and I. Ghosh, Molecules that target beta-amyloid, *ChemMedChem*, 2007, **2**, 1675–1692.
26 A. Lorenzo and B. A. Yankner, Beta-Amyloid neurotoxicity requires fibril formation and is inhibited by Congo Red, *Proc. Natl. Acad. Sci. U. S. A.*, 1994, **91**, 12243–12247.
27 E. N. Lee, H. J. Cho, C. H. Lee, D. Lee, K. C. Chung and S. R. Paik, Phthalocyanine tetrasulfonates affect the amyloid formation and cytotoxicity of alpha-synuclein, *Biochemistry*, 2004, **43**, 3704–3715.
28 L. Liu, L. Zhang, X. Mao, L. Niu, Y. Yang and C. Wang, Chaperon-Mediated single molecular approach toward modulating Aβ peptide aggregation, *Nano Lett.*, 2009, **9**, 4066–4072.
29 M. Harel, L. K. Sonoda, I. Silman, J. L. Sussman and T. L. Rosenberry, Crystal structure of thioflavin T bound to the peripheral site of Torpedo californica acetylcholinesterase reveals how thioflavin T acts as a sensitive fluorescent reporter of ligand binding to the acylation site, *J. Am. Chem. Soc.*, 2008, **130**, 7856–7861.
30 W. G. Turnell and J. T. Finch, Binding of the dye Congo Red to the amyloid protein pig insulin reveals a novel homology amongst amyloid-forming peptide sequences, *J. Mol. Biol.*, 1992, **227**, 1205–1223.
31 M. Biancalana, K. Makabe, A. Koide and S. Koide, Molecular mechanism of Thioflavin-T binding to the surface of beta-Rich peptide self-assemblies, *J. Mol. Biol.*, 2009, **385**, 1052–1063.
32 M. Groenning, L. Olsen, M. van de Weert, J. M. Flink, S. Frokjaer and F. S. Jorgensen, Study on the binding of Thioflavin T to beta-sheet-rich and non-beta-sheet cavities, *J. Struct. Biol.*, 2007, **158**, 358–369.
33 C. Wu, Z. X. Wang, H. X. Lei, W. Zhang and Y. Duan, Dual binding modes of Congo red to amyloid protofibril surface observed in molecular dynamics simulations, *J. Am. Chem. Soc.*, 2007, **129**, 1225–1232.
34 C. Wu, Z. X. Wang, H. X. Lei, Y. Duan, M. T. Bowers and J. E. Shea, The binding of Thioflavin T and its neutral analog BTA-1 to protofibrils of the Alzheimer's disease A beta(16–22) peptide probed by molecular dynamics simulations, *J. Mol. Biol.*, 2008, **384**, 718–729.
35 D. B. Carter and K. C. Chou, A model for structure-dependent binding of Congo red to Alzheimer beta-amyloid fibrils, *Neurobiol. Aging*, 1998, **19**, 37–40.
36 X. B. Mao, Y. B. Wang, L. Liu, L. Niu, Y. L. Yang and C. Wang, Molecular-level evidence of the surface-induced transformation of peptide structures revealed by scanning tunneling microscopy, *Langmuir*, 2009, **25**, 8849–8853.
37 R. Matmour, I. De Cat, S. J. George, W. Adriaens, P. Leclere, P. H. H. Bomans, N. A. J. M. Sommerdijk, J. C. Gielen, P. C. M. Christianen, J. T. Heldens, J. C. M. van Hest, D. W. P. M. Lowik, S. De Feyter, E. W. Meijer and A. P. H. J. Schenning, Oligo(p-phenylenevinylene)-peptide conjugates: Synthesis and self-assembly in solution and at the solid-liquid interface, *J. Am. Chem. Soc.*, 2008, **130**, 14576–14583.
38 A. Kühnle, T. R. Linderoth, B. Hammer and F. Besenbacher, Chiral recognition in dimerization of adsorbed cysteine observed by scanning tunnelling microscopy, *Nature*, 2002, **415**, 891–893.
39 M. Lingenfelder, G. Tomba, G. Costantini, L. C. Ciacchi, A. D. Vita and K. Kern, Tracking the chiral recognition of adsorbed dipeptides at the single-molecule level, *Angew. Chem., Int. Ed.*, 2007, **46**, 4492–4495.
40 X. B. Mao, X. J. Ma, L. Liu, L. Niu, Y. L. Yang and C. Wang, Structural characteristics of the beta-sheet-like human and rat islet amyloid polypeptides as determined by scanning tunneling microscopy, *J. Struct. Biol.*, 2009, **167**, 209–215.
41 X. Ma, L. Liu, X. Mao, L. Niu, K. Deng, W. Wu, Y. Li, Y. Yang and C. Wang, Amyloid-beta (1–42) folding multiplicity and single molecule binding behavior studied by STM, *J. Mol. Biol.*, 2009, **388**, 894–901.
42 C. G. Claessens, U. Hahn and T. Torres, Phthalocyanines: From outstanding electronic properties to emerging applications, *Chem. Rec.*, 2008, **8**, 75–97.
43 K. W. Hipps, L. Scudiero, D. E. Barlow, P. Manning and J. Cooke, A Self-organized 2-dimensional bifunctional structure formed by supramolecular design, *J. Am. Chem. Soc.*, 2002, **124**, 2126–2127.
44 S. B. Lei, C. Wang, S. X. Yin, H. N. Wang, F. Xi, H. W. Liu, B. Xu, L. J. Wan and C. L. Bai, Surface stabilized porphyrin and phthalocyanine two-dimensional network connected by hydrogen bonds, *J. Phys. Chem. B*, 2001, **105**, 10838–10841.
45 B. Xu, S. Yin, C. Wang, Q. Zeng, X. Qiu and C. Bai, Identification of hydrogen bond characterizations of isomeric 4Bpy and 2Bpy by STM, *Surf. Interface Anal.*, 2001, **32**, 245–247.
46 X. J. Ma, Y. T. Shen, K. Deng, H. Tang, S. B. Lei, C. Wang, Y. L. Yang and X. Z. Feng, Matrix-molecule induced chiral enhancement effect of binary supramolecular liquid crystals, *J. Mater. Chem.*, 2007, **17**, 4699–4704.
47 C. L. Claypool, F. Faglioni, W. A. Goddard, H. B. Gray, N. S. Lewis and R. A. Marcus, Source of image contrast in STM images of functionalized alkanes on graphite: A systematic functional group approach, *J. Phys. Chem. B*, 1997, **101**, 5978–5995.
48 D. Wintgens, D. G. Yablon and G. W. Flynn, Packing of $HO(CH2)_{14}COOH$ and $HO(CH2)_{15}COOH$ on graphite at the liquid-solid interface observed by scanning tunneling microscopy: Methylene unit direction of self-assembly structures, *J. Phys. Chem. B*, 2003, **107**, 173–179.
49 D. M. Cyr, B. Venkataraman, G. W. Flynn, A. Black and G. M. Whitesides, Functional group identification in scanning tunneling microscopy of molecular adsorbates, *J. Phys. Chem.*, 1996, **100**, 13747–13759.
50 K. Tsemekhman, L. Goldschmidt, D. Eisenberg and D. Baker, Cooperative hydrogen bonding in amyloid formation, *Protein Sci.*, 2007, **16**, 761–764.
51 B. Y. Ma and R. Nussinov, Simulations as analytical tools to understand protein aggregation and predict amyloid conformation, *Curr. Opin. Chem. Biol.*, 2006, **10**, 445–452.

52 J. J. W. Wiltzius, M. Landau, R. Nelson, M. R. Sawaya, M. I. Apostol, L. Goldschmidt, A. B. Soriaga, D. Cascio, K. Rajashankar and D. Eisenberg, Molecular mechanisms for protein-encoded inheritance, *Nat. Struct. Mol. Biol.*, 2009, **16**, 973–979.
53 M. R. Sawaya, S. Sambashivan, R. Nelson, M. I. Ivanova, S. A. Sievers, M. I. Apostol, M. J. Thompson, M. Balbirnie, J. J. W. Wiltzius, H. T. McFarlane, A. O. Madsen, C. Riekel and D. Eisenberg, Atomic structures of amyloid cross-beta spines reveal varied steric zippers, *Nature*, 2007, **447**, 453–457.
54 B. Raman, E. Chatani, M. Kihara, T. Ban, M. Sakai, K. Hasegawa, H. Naiki, C. M. Rao and Y. Goto, Critical balance of electrostatic and hydrophobic interactions is required for beta(2)-microglobulin amyloid fibril growth and stability, *Biochemistry*, 2005, **44**, 1288–1299.
55 V. Chauhan and A. Chauhan, Kinetics of formation of hydrophobic domains in fibrillar amyloid beta-protein, *FEBS J.*, 2005, **272**, 70–70.
56 R. D. Hills and C. L. Brooks, Hydrophobic cooperativity as a mechanism for amyloid nucleation, *J. Mol. Biol.*, 2007, **368**, 894–901.
57 D. E. Otzen, O. Kristensen and M. Oliveberg, Designed protein tetramer zipped together with a hydrophobic Alzheimer homology: A structural clue to amyloid assembly, *Proc. Natl. Acad. Sci. U. S. A.*, 2000, **97**, 9907–9912.
58 A. Quist, L. Doudevski, H. Lin, R. Azimova, D. Ng, B. Frangione, B. Kagan, J. Ghiso and R. Lal, Amyloid ion channels: A common structural link for protein-misfolding disease, *Proc. Natl. Acad. Sci. U. S. A.*, 2005, **102**, 10427–10432.
59 H. B. Jang, J. Zheng, R. Lal and R. Nussinov, New structures help the modeling of toxic amyloid beta ion channels, *Trends Biochem. Sci.*, 2008, **33**, 91–100.
60 L. Polo, G. Valduga, G. Jori and E. Reddi, Low-density lipoprotein receptors in the uptake of tumour photosensitizers by human and rat transformed fibroblasts, *Int. J. Biochem. Cell Biol.*, 2002, **34**, 10–23.
61 Y. Degani and I. Willner, Complex formation between anthraquinone-2,6-disulfonate and a neutral zinc porphyrin. Effects of CTAB micelles on complex stability and photoinduced electron transfer, *J. Phys. Chem.*, 1985, **89**, 5685–5689.
62 P. J. Muller and B. C. Wilson, Photodynamic therapy of brain tumors - A work in progress, *Lasers Surg. Med.*, 2006, **38**, 384–389.
63 B. W. Henderson and T. Dougherty, How does photodynamic therapy work, *Photochem. Photobiol.*, 1992, **55**, 145–157.
64 T. J. Dougherty, M. T. Cooper and T. S. Mang, Cutaneous phototoxic occurrences in patients receiving photofrin, *Lasers Surg. Med.*, 1990, **10**, 485–488.
65 T. J. Dougherty, C. J. Gomer, B. W. Henderson, G. Jori, D. Kessel, M. Korbelik, J. Moan and Q. Peng, Photodynamic therapy, *J. Natl. Cancer Inst.*, 1998, **90**, 889–905.
66 D. A. Bellnier, Y. K. Ho, R. K. Pandey, J. R. Missert and T. Dougherty, Distribution and Elimination of Photofrin-Ii in Mice, *Photochem. Photobiol.*, 1989, **50**, 221–228.
67 C. E. Giacomelli and W. Norde, Influence of hydrophobic Teflon particles on the structure of amyloid beta-peptide, *Biomacromolecules*, 2003, **4**, 1719–1726.
68 T. Vermonden, C. E. Giacomelli and W. Norde, Reversibility of structural rearrangements in bovine serum albumin during homomolecular exchange from AgI particles, *Langmuir*, 2001, **17**, 3734–3740.
69 M. Groenning, Binding mode of Thioflavin T and other molecular probes in the context of amyloid fibrils—current status, *J. Chem. Biol.*, 2009, **3**, 1–18.
70 W. L. DeLano, *The PyMOL User's Manual* (Delano Scientific, San Carlos, California, 2002).
71 Nanorex Inc., http://nanoengineer-1.com/content/.